Synthesis and Structural Characterization of a Highly Ordered Mesoporous Pt−Ru Alloy via "Evaporation-Mediated Direct Templating"

Yusuke Yamauchi,[†] Tetsu Ohsuna,[‡,§] and Kazuyuki Kuroda*[,†,‡,§]

Department of Applied Chemistry, Majors in Applied Chemistry and Nanoscience & Nanoengineering, Faculty of Science & Engineering, Waseda University, Ohkubo 3-4-1, Shinjuku-ku, Tokyo 169-8555, Japan, Kagami Memorial Laboratory for Materials Science and Technology, Waseda University, Nishi-waseda 2-8-26, Shinjuku-ku, Tokyo 169-0051, Japan, and CREST, Japan Science and Technology Agency, Honcho 4-1-8, Kawaguchi-shi, Saitama 332-0012, Japan

Received October 25, 2006. Revised Manuscript Received January 21, 2007

Highly ordered 2D-hexagonal mesoporous Pt−Ru alloy particles were deposited by an electrochemical process after a lyotropic liquid crystalline (LLC) film including both Pt and Ru species was prepared on a conductive substrate from a diluted surfactant solution by casting. We have determined the alloy state by using high-resolution scanning electron microscopy (HR-SEM), transmission electron microscopy (TEM), energy-dispersive X-ray spectroscopic (EDS) mapping, and X-ray photoelectron spectroscopy (XPS). The HR-SEM images show that the porous nanostructures are formed over the entire area on the external surface of each particle. The TEM images prove that the pore wall is composed of connected nanoparticles of ca. 3 nm in size and that the lattice fringes assigned to a fcc structure are randomly oriented. The EDS mapping shows both elements of Pt and Ru are well distributed within the pore wall. From the XPS data, Ru atoms in the alloy are thought to basically be in the zerovalent metallic state, Ru(0). These results indicate the formation of mesoporous intermetallic Pt−Ru alloys. The structural information on the mesoporous alloys should be very useful for development of mesoporous metals toward advanced nanomaterials.

Introduction

Since the discovery of mesoporous silica from kanemite (KSW-1),[1] mesoporous materials have attracted much attention for years because of the excellent physical properties (including a high specific surface area, uniform mesopores, periodic arrangement, and high stability) which are advantageous for catalysts, catalysis supports, inclusion vessels, and adsorbents.[2−9] The research area covers syntheses,[3] structural characterization,[4] morphological control (e.g., film, fiber, and monolith),[5] and alignment control of mesochannels.[6] Moreover, the compositions of pore walls have expanded into not only metal oxides but also carbon,[7] hybrid organosilicas,[8] and even polymers.[9] In 1997, Attard and co-workers successfully prepared mesoporous Pt (H_I-Pt) particles from lyotropic liquid crystals (LLC) made of surfactants self-assembled at high concentrations for the first time.[10] This pioneering work opened up a new field of metal-based mesoporous/mesostructured materials.[11] Mesoporous metals have been considered to have higher potentials than those of silica-based mesoporous materials in a wide range of electrochemical applications, such as electronic devices, magnetic devices, metal catalysts, and so on.[11] We have also adopted this concept and prepared mesoporous/mesostructured Ni[12] and Pt[13] with an enhanced ordering of mesostructure.

* Corresponding author. Fax and phone: +81-3-5286-3199. E-mail: kuroda@waseda.jp.

[†] Faculty of Science & Engineering, Waseda University.

[‡] Kagami Memorial Laboratory for Materials Science and Technology, Waseda University.

[§] CREST, Japan Science and Technology Agency.

(1) Yanagisawa, T.; Shimizu, T.; Kuroda, K.; Kato, C. *Bull. Chem. Soc. Jpn.* **1990**, *63*, 988−992.

(2) (a) Yanagisawa, T.; Shimizu, T.; Kuroda, K.; Kato, C. *Bull. Chem. Soc. Jpn.* **1990**, *63*, 1535−1537. (b) Kresge, C. T.; Leonowicz, M. E.; Roth, W. J.; Vartuli, J. C.; Beck, J. S. *Nature* **1992**, *359*, 710−712. (c) Beck, J. S.; Vartuli, J. C.; Roth, W. J.; Leonowicz, M. E.; Kresge, C. T.; Schmitt, K. D.; Chu, C. T. W.; Olson, D. H.; Sheppard, E. W.; Mccullen, S. B.; Higgins, J. B.; Schlenker, J. L. *J. Am. Chem. Soc.* **1992**, *114*, 10834−10843. (d) Inagaki, S.; Fukushima, Y.; Kuroda, K. *J. Chem. Soc., Chem. Commun.* **1993**, 680−682.

(3) (a) Inagaki, S.; Koiwai, A.; Suzuki, N.; Fukushima, Y.; Kuroda, K. *Bull. Chem. Soc. Jpn.* **1996**, *69*, 1449−1457. (b) Attard, G. S.; Goltner, C. G.; Corker, J. M.; Henke, S.; Templer, R. H. *Angew. Chem., Int. Ed. Engl.* **1997**, *36*, 1315−1317. (c) Monnier, A.; Schuth, F.; Huo, Q.; Kumar, D.; Margolese, D.; Maxwell, R. S.; Stucky, G. D.; Krishnamurty, M.; Petroff, P.; Firouzi, A.; Janicke, M.; Chmelka, B. F. *Science* **1993**, *261*, 1299−1303. (d) Huo, Q. S.; Margolese, D. I.; Ciesla, U.; Feng, P. Y.; Gier, T. E.; Sieger, P.; Leon, R.; Petroff, P. M.; Schuth, F.; Stucky, G. D. *Nature* **1994**, *368*, 317−321. (e) Bagshaw, S. A.; Prouzet, E.; Pinnavaia, T. J. *Science* **1995**, *269*, 1242−1244. (f) Che, S.; Liu, Z.; Ohsuna, T.; Sakamoto, K.; Terasaki, O.; Tatsumi, T. *Nature* **2004**, *429*, 281−284. (g) Zhang, Q.; Lü, F.; Li, C.; Wang, Y.; Wan, H. *Chem. Lett.* **2006**, *35*, 190−191.

(4) (a) Sakamoto, Y.; Kaneda, M.; Terasaki, O.; Zhao, D. Y.; Kim, J. M.; Stucky, G. D.; Shim, H. J.; Ryoo, R. *Nature* **2000**, *408*, 449−453. (b) Liu, Z.; Sakamoto, Y.; Ohsuna, T.; Hiraga, K.; Terasaki, O.; Ko, C. H.; Shin, H. J.; Ryoo, R. *Angew. Chem., Int. Ed.* **2000**, *39*, 3107−3110. (c) Shin, H. J.; Ryoo, R.; Liu, Z.; Terasaki, O. *J. Am. Chem. Soc.* **2001**, *123*, 1246−1247. (d) Guo, X. J.; Yang, C. M.; Liu, P. H.; Cheng, M. H.; Chao, K. J. *Cryst. Growth Des.* **2005**, *5*, 33−36.

(5) (a) Yang, H. F.; Shi, Q. H.; Tian, B. Z.; Xie, S. H.; Zhang, F. Q.; Yan, Y.; Tu, B.; Zhao, D. Y. *Chem. Mater.* **2003**, *15*, 536−541. (b) Takimura, M.; Nagata, H.; Yamasaki, Y.; Suzuki, T.; Ikuhara, Y.; Nakahira, A. *J. Ceram. Soc. Jpn.* **2006**, *114*, 554−557. (c) Xiong, L.; Nogami, M. *Chem. Lett.* **2006**, *35*, 972−973.

10.1021/cm062539n CCC: $37.00
Published on Web 02/22/2007

Moreover, "alloying of pore walls" has been focused as a key element for further developments to novel mesoporous metals with tunable functions and new solid-state properties. Several mesoporous alloys (e.g., Pt−Ru,[14] Pt−Pd,[15] Te−Cd,[16] Ni−Co,[17] Pt−Ni[18]) have been prepared by coreduction of two-metal species in the presence of LLC. In the cases of mesoporous Pt−Pd,[15] Te−Cd,[16] and Ni−Co,[17] it has been considered that nanoscale phase separations of the constituent metals occur in the pore walls. In contrast, the pore walls of mesoporous Pt−Ru[14] and Pt−Ni[18] are composed of binary intermetallic states, that is, the uniform dispersion of the constituent metals. It is well-known from the binary alloy phase diagrams that bulk Pt−Ru and Pt−Ni alloys take intermetallic states at room temperature.[19] In the case of mesoporous Pt−Ru, the "intermetallic state" has been proved by high-angle XRD and extended X-ray absorption fine structure (EXAFS).[14] Very recently, we have characterized the "intermetallic state" of mesoporous Pt−Ni by TEM, selected-area ED patterns, EDS mapping, and XPS analysis.[18] The Pt-based intermetallic alloys (e.g., Pt−Ru, Pt−Ni) have recently attracted great interest as candidates for electrode materials for the oxygen reduction reaction (ORR).[20] The improvement in ORR is explained by several factors, such as surface structural and electronic effects.[20] Therefore, a deeper understanding on the "alloy state" in the pore walls is of considerable importance from the viewpoint of applications of mesoporous alloys. This is also highly useful for obtaining new insights into the bath conditions governing the grain growth of alloy deposition within the limited space in LLC.

In this study, we have conclusively characterized highly ordered mesoporous Pt−Ru alloy particles with a 2D-hexagonal symmetry by using HR-SEM, TEM, ED, EDS mapping, and XPS analysis. Highly ordered mesoporous Pt−Ru alloys, having both high specific surface areas and uniform distribution of metals, will have an impact on a wide range of fields. Moreover, we applied the modified liquid-crystal templating method through solvent evaporation to deposit mesoporous Pt−Ru alloy onto a planar substrate,

(6) (a) Miyata, H.; Kuroda, K. *Chem. Mater.* **2000**, *12*, 49−54. (b) Miyata, H.; Kuroda, K. *Chem. Mater.* **1999**, *11*, 1609−1614. (c) Yamauchi, Y.; Sawada, M.; Noma, T.; Ito, H.; Furumi, S.; Sakka, Y.; Kuroda, K. *J. Mater. Chem.* **2005**, *15*, 1137−1140. (d) Yamauchi, Y.; Sawada, M.; Sugiyama, A.; Osaka, T.; Sakka, Y.; Kuroda, K. *J. Mater. Chem.* **2006**, *16*, 3693−3700. (e) Miyata, H.; Kawashima, Y.; Itoh, M.; Watanabe, M. *Chem. Mater.* **2005**, *17*, 5323−5327. (f) Noma, T.; Takada, K.; Miyata, H.; Iida, A. *Nucl. Instrum. Methods Phy. Res., Sect. A* **2001**, *467*, 1021−1025. (g) Miyata, H.; Suzuki, T.; Fukuoka, A.; Sawada, T.; Watanabe, M.; Noma, T.; Takada, K.; Mukaide, T.; Kuroda, K. *Nat. Mater.* **2004**, *3*, 651−656. (h) Tanaka, S.; Hillhouse, H. W. *Chem. Lett.* **2006**, *35*, 928−929. (i) Fukumoto, H.; Nagano, S.; Seki, T. *Chem. Lett.* **2006**, *35*, 180−181. (j) Yamada, T.; Zhou, H.; Honma, I.; Ueno, Y.; Horiuchi, T.; Niwa, O. *Chem. Lett.* **2005**, *34*, 328−329.

(7) (a) Joo, S. H.; Choi, S. J.; Oh, I.; Kwak, J.; Liu, Z.; Terasaki, O.; Ryoo, R. *Nature* **2001**, *412*, 169−172. (b) Choi, M.; Ryoo, R. *Nat. Mater.* **2003**, *2*, 473−476. (c) Vinu, A.; Ariga, K. *Chem. Lett.* **2005**, *34*, 674−675.

(8) (a) Inagaki, S.; Guan, S.; Fukushima, Y.; Ohsuna, T.; Terasaki, O. *J. Am. Chem. Soc.* **1999**, *121*, 9611−9614. (b) Asefa, T.; MacLachan, M. J.; Coombs, N.; Ozin, G. A. *Nature* **1999**, *402*, 867−871. (c) Inagaki, S.; Guan, S.; Ohsuna, T.; Terasaki, O. *Nature* **2002**, *416*, 304−307. (d) Ohtani, O.; Goto, Y.; Okamoto, K.; Inagaki, S. *Chem. Lett.* **2005**, *34*, 1342−1343. (e) Zhang, Z.; Yan, X.; Tian, B.; Shen, S.; Chen, D.; Zhu, G.; Qiu, S.; Zhao, D. *Chem. Lett.* **2005**, *34*, 182−183.

(9) (a) Meng, Y.; Gu, D.; Zhang, F. Q.; Shi, Y. F.; Yang, H. F.; Li, Z.; Yu, C. Z.; Tu, B.; Zhao, D. Y. *Angew. Chem., Int. Ed.* **2005**, *44*, 7053−7059. (b) Liu, R. L.; Shi, Y. F.; Wan, Y.; Meng, Y.; Zhang, F. Q.; Gu, D.; Chen, Z. X.; Tu, B.; Zhao, D. Y. *J. Am. Chem. Soc.* **2006**, *128*, 11652−11662. (c) Zhang, F. Q.; Meng, Y.; Gu, D.; Yan, Y.; Yu, C. Z.; Tu, B.; Zhao, D. Y. *J. Am. Chem. Soc.* **2005**, *127*, 13508−13509.

(10) Attard, G. S.; Göltner, C. G.; Corker, J. M.; Henke, S.; Templer, R. H. *Angew. Chem., Int. Ed.* **1997**, *36*, 1315−1317.

(11) (a) Attard, G. S.; Bartlett, P. N.; Coleman, N. R. B.; Elliott, J. M.; Owen, J. R.; Wang, J. H. *Science* **1997**, *278*, 838−840. (b) Whitehead, A. H.; Elliott, J. M.; Owen, J. R.; Attard, G. S. *Chem. Commun.* **1999**, 331−332. (c) Nelson, P. A.; Elliott, J. M.; Attard, G. S.; Owen, J. R. *Chem. Mater.* **2002**, *14*, 524−529. (e) Luo, H. M.; Sun, L.; Lu, Y. F.; Yan, Y. S. *Langmuir* **2004**, *20*, 10218−10222. (f) Boo, H.; Park, S.; Ku, B. Y.; Kim, Y.; Park, J. H.; Kim, H. C.; Chung, T. D. *J. Am. Chem. Soc.* **2004**, *126*, 4524−4525. (g) Elliott, J. M.; Attard, G. S.; Bartlett, P. N.; Coleman, N. R. B.; Merckel, D. A. S.; Owen, J. R. *Chem. Mater.* **1999**, *11*, 3602−3609. (h) Jiang, J.; Kucernak, A. *J. Electroanal. Chem.* **2002**, *520*, 64−70. (i) Jiang, J.; Kucernak, A. *J. Electroanal. Chem.* **2002**, *533*, 153−165. (j) Kucernak, A.; Jiang, J. *Chem. Eng. J.* **2003**, *93*, 81−91. (k) Kijima, T.; Yoshimura, T.; Uota, M.; Ikeda, T.; Fujikawa, D.; Mouri, S.; Uoyama, S. *Angew. Chem., Int. Ed.* **2003**, *43*, 228−232.

(12) (a) Yamauchi, Y.; Yokoshima, T.; Mukaibo, H.; Tezuka, M.; Shigeno, T.; Momma, T.; Osaka, T.; Kuroda, K. *Chem. Lett.* **2004**, *33*, 542−543. (b) Yamauchi, Y.; Momma, T.; Yokoshima, T.; Kuroda, K.; Osaka, T. *J. Mater. Chem.* **2005**, *15*, 1987−1994. (c) Yamauchi, Y.; Yokoshima, T.; Momma, T.; Osaka, T.; Kuroda, K. *Electrochem. Solid-State. Lett.* **2005**, *8*, C141−C144.

(13) (a) Yamauchi, Y.; Yokoshima, T.; Momma, T.; Osaka, T.; Kuroda, K. *Chem. Lett.* **2004**, *33*, 1576−1577. (b) Yamauchi, Y.; Momma, T.; Fuziwara, M.; Sivakumar Nair, S.; Ohsuna, T.; Terasaki, O.; Osaka, T.; Kuroda, K. *Chem. Mater.* **2005**, *17*, 6342−6348.

(14) (a) Attard, G. S.; Leclerc, S. A. A.; Maniquet, S.; Russell, A. E.; Nandhakumar, I.; Bartlett, P. N. *Chem. Mater.* **2001**, *13*, 1444. (b) Jiang, J. H.; Kucernak, A. *J. Electroanal. Chem.* **2003**, *543*, 187−199. (c) Jiang, J. H.; Kucernak, A. *Chem. Mater.* **2004**, *16*, 1362−1367. (d) Attard, G. S.; Leclerc, S. A. A.; Maniguet, S.; Russell, A. E.; Nandhakumar, I.; Gollas, B. R.; Bartlett, P. N. *Microporous Mesoporous Mater.* **2001**, *44*, 159−163.

(15) Guerin, S.; Attard, G. S. *Electrochem. Commun.* **2001**, *3*, 544−548.

(16) (a) Nandhakumar, I. S.; Gabriel, T.; Li, X.; Attard, G. S.; Markham, M.; Smith, D. C.; Baumberg, J. J. *Chem. Commun.* **2004**, 1374−1375. (b) Markham, M. L.; Baumberg, J. J.; Smith, D. C.; Li, X.; Gabriel, T.; Attard, G. S.; Nandhakumar, I. *Appl. Phys. Lett.* **2005**, *86*, 011912. (c) Li, X.; Nandhakumar, I. S.; Gabriel, T.; Attard, G. S.; Markham, M. L.; Smith, D. C.; Baumberg, J. J.; Govender, K.; O'Brienc, P.; Smyth-Boyle, D. *J. Mater. Chem.* **2006**, *16*, 3207−3214.

(17) (a) Yamauchi, Y.; Yokoshima, T.; Momma, T.; Osaka, T.; Kuroda, K. *J. Mater. Chem.* **2004**, *14*, 2935−2940. (b) Yamauchi, Y.; Sadasivan Nair, S.; Yokoshima, T.; Momma, T.; Osaka, T.; Kuroda, K. *Stud. Surf. Sci. Catal.* **2005**, *156*, 457−464.

(18) Yamauchi, Y.; Sivakumar, Nair, S.; Momma, T.; Ohsuna, T.; Osaka, T.; Kuroda, K. *J. Mater. Chem.* **2006**, *16*, 2229−2234.

(19) *Binary Alloy Phase Diagrams*, 2nd ed.; Massalski, T. B., Subramanian, P. R., Kacprzak, L., Eds.; ASM International: Materials Park, OH, 1996.

(20) (a) Lasch, K.; Jorissen, L.; Garche, J. *J. Power Sources* **1999**, *84*, 225−230. (b) Cattaneo, C.; de Pinto, M. I. S.; Mishima, H.; de Mishima, B. A. L.; Lescano, D.; Cornaglia, L. *J. Electroanal. Chem.* **1999**, *461*, 32−39. (c) Liu, R. X.; Iddir, H.; Fan, Q. B.; Hou, G. Y.; Bo, A. L.; Ley, K. L.; Smotkin, E. S.; Sung, Y. E.; Kim, H.; Thomas, S.; Wieckowski, A. *J. Phys. Chem. B* **2000**, *104*, 3518−3531. (d) Park, K. W.; Choi, J. H.; Kwon, B. K.; Lee, S. A.; Sung, Y. E.; Ha, H. Y.; Hong, S. A.; Kim, H.; Wieckowski, A. *J. Phys. Chem. B* **2002**, *106*, 1869−1877. (e) Motokawa, S.; Mohamedi, M.; Momma, T.; Shoji, S.; Osaka, T. *Electrochem. Commun.* **2004**, *6*, 562−565. (f) Motokawa, S.; Mohamedi, M.; Momma, T.; Shoji, S.; Osaka, T. *Electrochemistry* **2005**, *73*, 346−351. (g) Motokawa, S.; Obata, H.; Mohamedi, M.; Momma, T.; Shoji, S.; Osaka, T. *Electrochemistry* **2005**, *73*, 352−355. (h) Liu, Z. L.; Ling, X. Y.; Su, X. D.; Lee, J. Y.; Gan, L. M. *J. Power Sources* **2005**, *149*, 1−7. (i) Huang, J. C.; Liu, Z. L.; He, C. B.; Gan, L. M. *J. Phys. Chem. B* **2005**, *109*, 16644−16649. (j) Aricò, A. S.; Cretì, P.; Kim, H.; Mantegna, R.; Giordano, N.; Antonuccia, V. *J. Electrochem. Soc.* **1996**, *143*, 3950−3959. (k) Yang, L. X.; Allen, R. G.; Scott, K.; Christensen, P.; Roy, S. *J. Fuel Cell Sci. Technol.* **2005**, *2*, 104−110. (l) Allen, R. G.; Lim, C.; Yang, L. X.; Scott, K.; Roy, S. *J. Power Sources* **2005**, *143*, 142−149. (m) Yang, L. X.; Allen, R. G.; Scott, K.; Christenson, P.; Roy, S. *J. Power Sources* **2004**, *137*, 257−263. (n) Bauer, A.; Gyenge, E. L.; Oloman, C. W. *Electrochim. Acta* **2006**, *51*, 5356−5364.

Figure 1. Photograph of a diluted surfactant solution (precursor solution) as an LLC former.

though this method was originally developed for fabrication of mesoporous metals into a very confined space.[21] Another advantageous point of this method is that the LLC templating mixture can be directly formed from a diluted surfactant solution (precursor solution) without heating-aging processes which have been commonly used in the general synthesis of mesoporous metals.[10−18] The present evaporation process[21] is quite different from the conventional "evaporation-induced self-assembly" (EISA) method. The details on the difference will be discussed later.

Experimental Procedures

Materials. Nonionic surfactant ($C_{16}H_{33}(OCH_2CH_2)_8OH$, $C_{16}EO_8$, octaethylene glycol monohexadecyl ether) was purchased from Aldrich Co. Hydrogen hexachloroplatinate(IV) hydrate (79.3% as H_2PtCl_6, as determined by ICP, Kanto Kagaku Co.) and hydrated ruthenium(III) trichloride (92.5% as $RuCl_3$, as determined by ICP, Kanto Kagaku Co.) were used as Pt and Ru sources, respectively. Ethanol (H_2O content <0.005%, Wako Chemical Co.) was used both for dilution of the precursor solution and for removal of templates.

Formation of LLC from a Diluted Surfactant Solution. A diluted surfactant solution (precursor solution) as a LLC former was prepared by mixing distilled water (0.15 g), nonionic surfactant $C_{16}EO_8$ (0.21 g), hydrogen hexachloroplatinate(IV) hydrate (0.072 g), hydrated ruthenium(III) trichloride (0.035 g), and ethanol (3.00 mL) as a volatile solvent. The mole ratio of platinum to ruthenium was 48:52 (nominal 1:1). The precursor solution was stirred for 10 min at room temperature and became a homogeneous dark brown solution with low viscosity (Figure 1). The precursor solution was cast onto a Au-coated Si substrate and then dried at 25 °C for 1 h. After the volatile solvent was preferentially evaporated, an LLC film including both Pt and Ru species was entirely formed on the substrate. The thickness of the LLC film was ca. 0.5 mm. For the preparation of the Au-coated Si substrate, Ti and Au for current collectors were uniformly coated onto a Si substrate by vacuum deposition. A 100 nm Au layer was deposited in an ULVAC CRTM-6000 electron beam evaporation chamber, preceded by the deposition of a 20 nm Ti layer just beneath the gold to promote the adhesion with the surface of silicon dioxide.

Electrochemical Deposition of Mesoporous Pt−Ru Alloy Particles. Electrochemical depositions were carried out for 12 h at room temperature at a constant potential (−0.10 V vs Ag/AgCl) by using a potentiostat/galvanostat HA-151 (Hokuto Denko Corp.). A Pt-coated Si substrate as a counter electrode was put onto the LLC-modified substrate to sandwich the LLC. The sandwiched LLC can suppress the evaporation of water molecules which may affect the structures of LLC mesophases.[22] The electrode distance between the working and counter electrodes was fixed by using a PTFE (poly(tetrafluoroethylene)) separator. A Ag/AgCl electrode was used as a reference electrode. The reference electrode was connected to LLC by using a salt bridge. In this study, the deposition area was fixed to be 0.5 mm × 0.5 mm, providing a uniform distribution of current density on the working electrode. It allows metals to be uniformly deposited on the substrate surface. After deposition, mesostructured Pt−Ru was placed in ethanol and deionized water for 2 d to extract $C_{16}EO_8$ and to remove undeposited metal species, and the extraction procedure was repeated 3−4 times. The solution after the extraction showed a homogeneous dark brown color, meaning that undeposited Ru(III) and Pt(IV) species were dissolved in the solution.

Characterization. The liquid crystalline state of the templating mixtures on a glass slide was confirmed by an Olympus BX-51 optical microscope under a crossed Nicol field, and the image was recorded on a digital camera (Canon IXY DIGITAL 800 IS). XRD patterns at lower diffraction angles were measured with a Mac Science M03XHF22 diffractometer with Mn-filtered Fe Kα radiation (40 kV, 20 mA) at a scanning rate of 0.5°/min. SEM images were obtained using a Hitachi HR-SEM S-5500 microscope operating at 20 kV. Samples were observed directly without any coatings. TEM images were taken by a JEOL JEM-ARM1250 microscope using an accelerating voltage of 1250 kV. Powder samples for the TEM observation were scratched from the substrate and then dispersed in ethanol by ultrasound and mounted on a carbon-coated microgrid (Okenshoji Co.). EDS mapping was performed by a JEM-3000F transmission electron microscope using an accelerating voltage of 300 kV. XPS analysis was carried out to conclusively investigate the electronic states of the surface of the mesoporous Pt−Ru alloys. XPS spectra were taken at room temperature using an ESCA Lab-200R instrument with a Mg Kα X-ray source. All binding energies were calibrated by referencing Au $4f_{7/2}$ (84.0 eV).

Results and Discussion

Formation of LLC Film from a Diluted Surfactant Solution. Figure 1 shows the photograph of the diluted surfactant solution containing Pt and Ru species. The homogeneous precursor solution is composed of soluble Pt and Ru species and nonionic surfactant dissolved in water and ethanol. The viscosity of the diluted surfactant solution is very low in comparison with those of general LLC templating mixtures[10−18] prepared by heating-aging processes. For the preparation of the LLC film, the precursor solution with low viscosity was cast onto a substrate and dried to form an LLC mesophase. Figure 2 shows the polarized optical microscopic images for in-situ observation. At an initial stage, liquid crystallinity cannot be observed at all. As ethanol was progressively evaporated, liquid crystallinity

(21) (a) Yamauchi, Y.; Momma, T.; Kitoh, H.; Osaka, T.; Kuroda, K. *Electrochem. Commun.* **2005**, *7*, 1364−1370. (b) Yamauchi, Y.; Kitoh, H.; Momma, T.; Osaka, T.; Kuroda, K. *Sci. Technol. Adv. Mater.* **2006**, *7*, 438−445. (c) Yamauchi, Y.; Kuroda, K. *Electrochem. Commun.* **2006**, *8*, 1677−1682.

(22) (a) Çelik, Ö.; Dag, Ö. *Angew. Chem., Int. Ed.* **2001**, *40*, 3800−3803. (b) Dag, Ö.; Samarskaya, O.; Tura, C.; Gunay, A.; Çelik, Ö. *Langmuir* **2003**, *19*, 3671−3676. (c) Dag, Ö.; Alayoglu, S.; Uysal. *J. Phys. Chem. B* **2004**, *108*, 8439−8446.

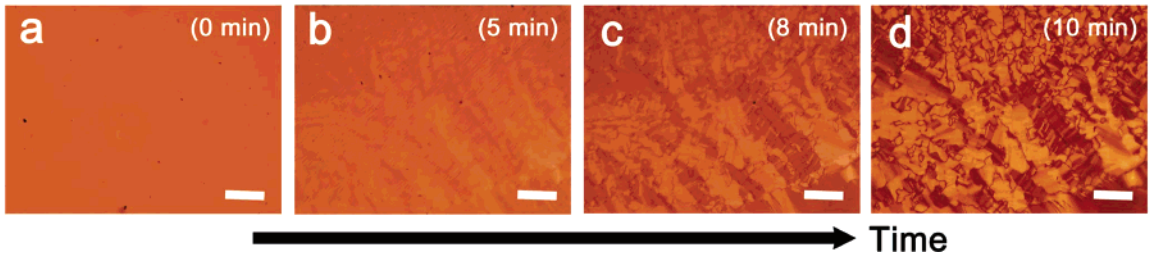

Figure 2. Polarized optical microscopic images: (a) diluted surfactant solution; (b−d) time-dependent change of liquid crystallinity. Scale bar: 100 μm.

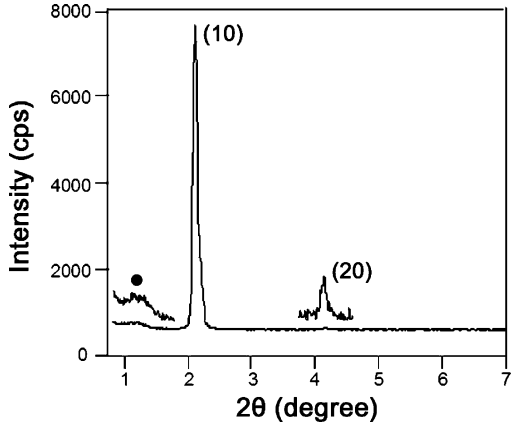

Figure 3. Low-angle XRD pattern of the LLC templating mixture prepared on the substrate through solvent evaporation. The extra peak is indicated by a filled circle (●).

appeared (Figure 2b) and gradually grew (Figure 2c,d). Figure 2d shows a typical fanlike texture which is a representative feature of 2D-hexagonal (H_I) LLC mesophase, (The determination by low-angle XRD is described in the next paragraph.) The domain size of a single phase in the LLC was estimated to be larger than 100 μm (Figure 2d). On the basis of these results, it is proved that the preferential evaporation of ethanol accelerates to form LLC mesophases including Pt and Ru species; that is, the progressive increase of surfactant concentration drives the self-organization of surfactants to make the LLC mesophases.

In the "*direct templating*" utilizing LLC, the deposited mesostructures can be directly determined by the structures of used LLC mesophases.[10−18,21] Therefore, the structural determination of LLC mesophases which are formed from diluted solutions is required. The low-angle XRD pattern of the LLC film shows two diffraction peaks (d_{10} = 5.6 nm, d_{20} = 2.8 nm). These two peaks can be assigned to be (10) and (20) in a 2D-hexagonal (*p*6*mm*) symmetry with a lattice parameter of 6.5 nm (Figure 3). The absence of the (11) peak indicates that the formed LLC phase has some domains in which rodlike self-assemblies are parallel to the substrate surface and that the (10) face is aligned parallel to the substrate. The same behavior has often been observed in continuous mesoporous silica films.[6a−e] An extra peak, marked "●" in Figure 3, was observed at $2\theta = 1.4°$ (d = 12 nm), and this spacing is about twice that of the d_{10} value. Though the spacing is forbidden for a 2D-hexagonal structure, the extra peak is ascribed to the reciprocal lattice point which does not appear in a conventional $\theta-2\theta$ scanning XRD measurement under an ideal measurement condition.[6a−f] It has been already demonstrated, by Noma and Miyata et al., that the vertical divergence of the incident beam and the small diffraction angle made the reciprocal lattice point detectable.[6a−f] The use of such a high-quality LLC as a starting material must play a key role for the formation of highly ordered mesoporous structures with a 2D-hexagonal (*p*6*mm*) symmetry.

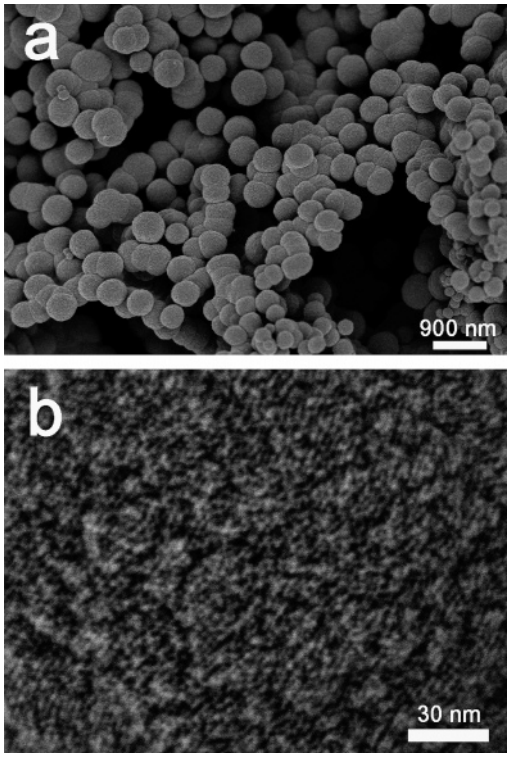

Figure 4. (a) Low-magnified SEM image of mesoporous Pt−Ru alloy particles and (b) highly magnified SEM image of the external surface of one particle.

Structural Characterization of Mesoporous Pt−Ru Alloy Synthesized from LLC Film. Figure 4 shows the SEM images of mesoporous Pt−Ru alloy particles deposited on the substrate. The low magnified SEM image shows that the deposits consist of aggregated spherical particles (Figure 4a). The particle size distribution is in the range 50−800 nm. The highly magnified SEM images of the external surfaces on each particle show the presence of both periodically arranged mesopores and the uniform arrays of mesochannels (Figure 4b). The mesopores observed at the external surface are open, which should provide a pathway for high diffusion.

The surface morphologies of the deposited films strongly depend on the experimental conditions, in particular deposition potentials, which has already been reported by Attard et al.[11g] and Kucernak et al.[14c] At low overpotentials, the obtained films show remarkably smooth surfaces, and the existence of the assembled surfactants would act as a leveling

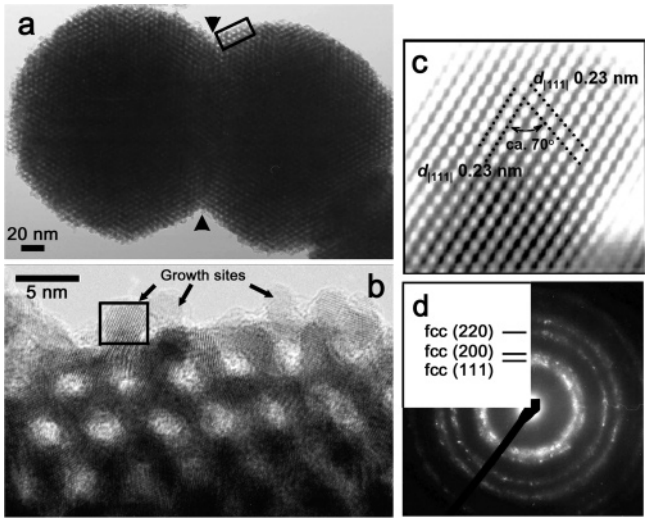

Figure 5. TEM images and selected ED pattern of mesoporous Pt−Ru alloy particles: (a) low-magnified TEM image; (b) highly magnified TEM image of the square area in image a; (c) a filtered image of the square area in image b; (d) selected-area ED pattern in 100 nm range of right particle in image a.

agent.[11a,14c] On the other hand, as overpotentials during metal depositions become higher, the surface becomes rougher in texture, i.e., aggregation of particles (see Figure 7a in ref 14c).[14c] The nucleation reaction relatively tends to proceed in comparison with the grain growth reaction. It has already been explained that such a formation of aggregated particles is also induced by low diffusion of metal species during metal deposition and high viscosities of electrolytes.[23] The experimental conditions used in this study are suitable to form such aggregated particles. Under the kinetic control at low overpotentials, continuous mesoporous films with smooth surface may be realized. The factors such as concentration of metal species and viscosity of electrolyte would also play important key roles for the selective formation of continuous films and aggregated particles.

Two types of TEM images of the same aggregated particles (Figure S1a,b) were taken by changing tilt angles. The pore−pore distance is found to be ca. 6 nm, which is close to the lattice parameter (6.5 nm) of the LLC film. Even at the interface between the particles, the honeycomb structure was retained, as indicated by arrows (Figures S1a and 5a). The mesochannels within several connected particles run parallel in one direction like a bundle of strings (Figures S1b and S2), indicating that the particles were formed within the same single domain of LLC. Such macroscopic alignments can be achieved only by the real "*direct templating*".[12c] These macroscopic alignments of mesochannels reflect those of rodlike self-assemblies in LLC mesophase, as is explained as follows. The size of one particle was from 50 to 800 nm from SEM observation (Figure 4a), while a single domain of the LLC was larger than 100 μm from the polarized optical microscopic image (Figure 2d). In each single domain, the rodlike self-assemblies of surfactants are uniaxially oriented parallel to the substrate in the same directions. The size of one particle is much smaller than that of a single domain of the original LLC. Therefore, several connected particles, shown in Figure 4a, are expected to be deposited in the same domain. The Pt−Ru deposition was carried out among the oriented rodlike self-assemblies, resulting in the formation of macroscopic alignment derived from the LLC. The alloy prepared via our method has a long-range ordering of the mesoporous structure. Interconnections of mesochannels at the interface between particles were observed for mesoporous Pt−Ru alloy with the LLC templating mixture prepared by heating-aging processes[14] (especially see Figure 3 in ref 14c), but the real direct templating was clearly observed here, by using a high-quality LLC and applying the optimized deposition condition.

We investigated further the detailed microstructure of the framework at higher magnification (Figures 5 and S3). The framework shows a bumpy morphology (Figure 5b). Several growth sites that can be interpreted as nucleation sites on the external surface were also highlighted (Figure 5b). The TEM image shows that the pore wall is composed of connected nanoparticles with an average size of ca. 3 nm (Figures 5b and S3). This formation of the similar connected nanoparticles was also observed in mesoporous Pt particles from LLC prepared with the same nonionic surfactant (C_{16}-EO_8). Connected nanoparticles have been reported to be formed by the unique deposition of the metals in soft-templates of LLC.[13b] The lattice fringes on one nanoparticle correspond to the {111} planes because both *d*-spacings are ca. 0.23 nm and the dihedral angle is ca. 70° (Figure 5c). Each nanoparticle has single crystallinity with a fcc structure.

The selected-area ED pattern from a 100 nm region shows the ring pattern assigned to a fcc structure. The presence of other phases (e.g., $PtRu_3$ and PtRu (ordered structures), Ru oxides) was not confirmed (Figure 5d). The lattice fringes are randomly oriented across over the connected nanoparticles. The observed ED pattern is constituted of diffused rings and intense points located on the rings. As indicated by the arrows in Figure S3, the size of the domains with the single atomic crystallinity are various, from 3 to 10 nm (or larger) (equal to 1−3 nanoparticles or more). We consider that the recording of the intense diffraction points is attributed to the coexistence of such larger crystals.

It should be noted that the domain size is remarkably small compared to that of mesoporous Pt particles from LLC prepared by using the same surfactant,[13b] though the synthetic conditions are quite different. The codeposition of two metal species, having different standard electrode potentials (E_0) (Pt, 1.19 V; Ru, 0.46 V[24]), may affect the reduction of the domain size of the single atomic crystallinity. It has already been reported that electrodeposited Pt-group alloy nanoparticles (e.g., Pt−Ru, Pt−Ru−Ni) prepared in the absence of surfactants possess smaller atomic crystalline size compared to Pt alone (see Figure 1 in ref 20d). The same phenomena have also been observed, when other processes (e.g., microwave-assisted polyol process, hydrosilylation process) were applied (see Figure 4 in ref 20h and Figure 4 in ref 20i).

(23) Pletcher, D.; Walsh, F. *Industrial Electrochemistry*, 2nd ed.; Chapman & Hall: London, 1990.

(24) *Tables of Standard Electrode Potentials*; Milazzo, G., Caroli, S., Eds.; John Wiley & Sons, Ltd.: New York, 1978.

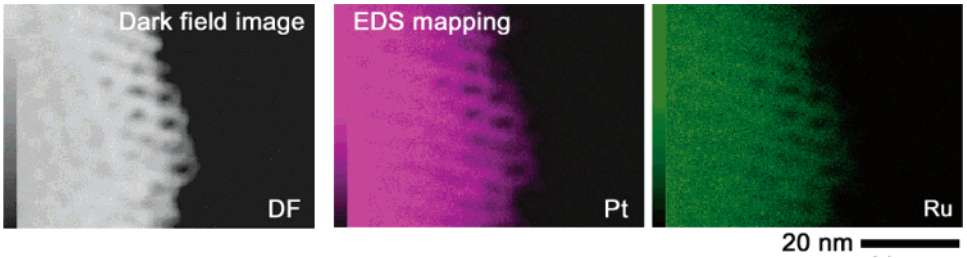

Figure 6. EDS mapping of mesoporous Pt−Ru alloy particle: dark-field (DF) image and the elemental distributions of Pt and Ru. Scale bar: 20 nm.

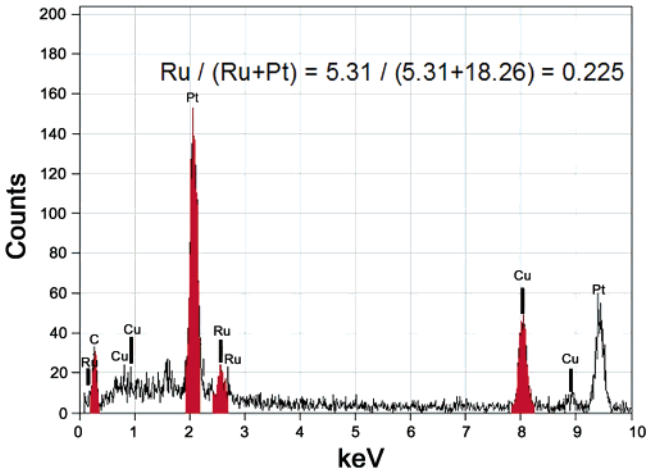

Figure 7. EDS spectrum of mesoporous Pt−Ru alloy particles.

Figure 6 shows the EDS mapping of the mesoporous Pt−Ru alloy particles. The dark field (DF) STEM image completely corresponds to the images of the EDS mapping of Pt and Ru. The Pt and Ru atoms are well-dispersed within the pore wall. No phase separations in a nanometer scale were observed. This EDS mapping shown here is the first direct evidence that the pore wall is composed of a binary intermetallic state, that is, a uniform dispersion of the constituent metals.

Figure 7 shows the EDS spectrum of the mesoporous Pt−Ru alloy particles. The composition ratio was measured to be Pt:Ru = 77:23. The Pt was preferentially deposited in the presence of LLC, because of the difference of the standard electrode potentials of Pt and Ru.[24] Previous reports on mesoporous Pt−Ni and Pt−Pd alloys also show that Pt was preferentially deposited, because the standard electrode potentials of Ni and Pd are 0.26 and 0.92 V, respectively.[24] The other peaks assigned to be C (carbon) and Cu (copper) were due to a carbon microgrid and a copper mesh, respectively. Most importantly, a notable signal assigned to oxygen did not appear. Though the sensitivity of light element (oxygen) in EDS analysis is low, it is suggested that both Pt and Ru are basically not oxidized. The selected-area ED pattern (Figure 5d) also indicates no formation of both RuO_2 and other Ru oxide compounds.

The XPS spectrum of Pt 4f of mesoporous Pt−Ru alloy is shown in Figure 8a. The Pt $4f_{7/2}$ and $4f_{5/2}$ spectra were observed at 71.0 and 74.5 eV, respectively. These values of Pt 4f peaks were very close to 70.9 and 74.2 eV for bulk Pt metal.[25] The results suggest that Pt is present in the zerovalent state. Regarding the electronic states of Ru, the XPS spectrum was measured in the energy region (450−490 eV) where Ru 3p peaks are expected to appear, because the Ru 3d region

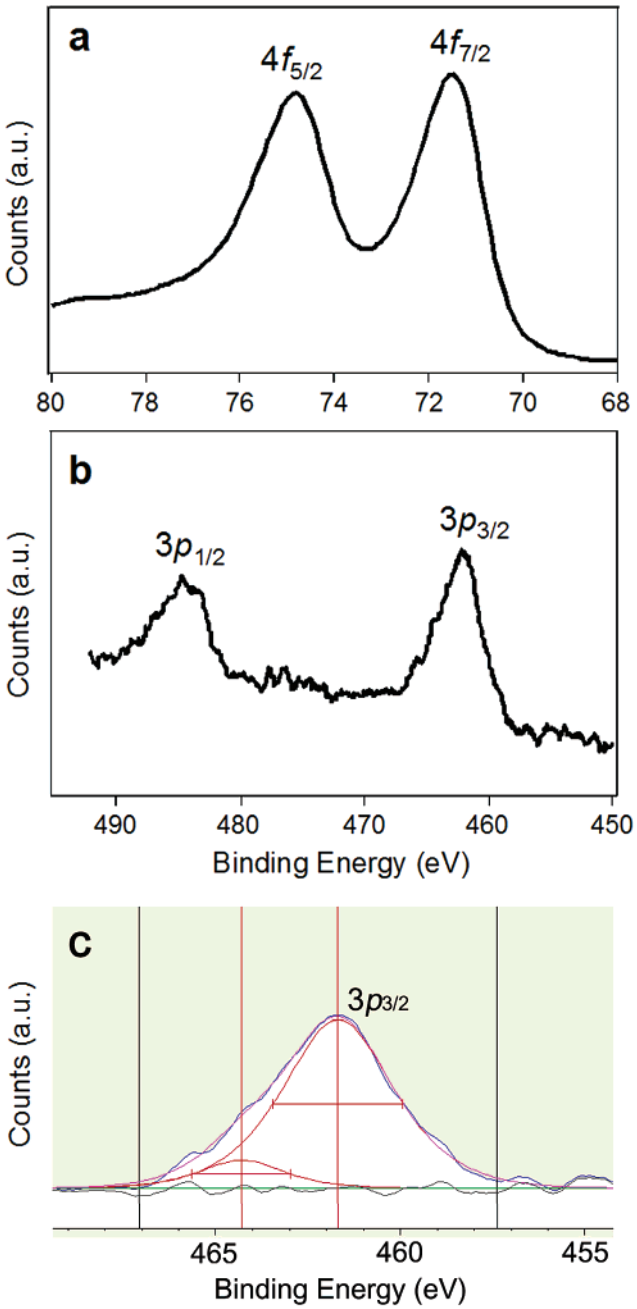

Figure 8. (a) XPS spectrum of Pt, (b) XPS spectrum of Ru, and (c) deconvolution of the Ru $3p_{3/2}$ signal by using a Gaussian−Lorenz function.

is often obscured by the strong C 1s signal due to surface contamination by carbon (Figure 8b). The Ru $3p_{3/2}$ signal was deconvoluted into two peaks with different intensities

(25) Wagner, C. D.; Riggs, W. M.; Davis, L. E.; Moulder, J. F. In *Handbook of X-ray Photoelectron Spectroscopy*; Mullemberg, G. E., Ed.; Perkin-Elmer: Eden Prairie, MN, 1978.

by using a Gaussian−Lorenz function (Figure 8c). The main peak was located at 461.8 eV which is assigned to Ru(0).[25] The fwhm of the peak is about 3.5 eV, and the value is similar to that of bulk Ru(0) reported in a previous report.[20a] The other peak at higher energy (464.2 eV) may be attributed to Ru oxide phases such as RuO_2 and RuO_3.[20a] On the basis of the peak areas, it is proved that more than 90 at. % Ru is present in the zerovalent state. Though it is well-known that Ru in nanosize is easily oxidized in air, it is important to note that the Ru on the surface of mesoporous Pt−Ru alloy is basically present in a zerovalent state. In the previous studies on bulk Pt−Ru alloys by other methods, it has been reported that Ru is present in the zerovalent state.[20b,c,i] The surface compositional ratio (Pt:Ru) was estimated to be about 80:20 on the basis of the peak areas due to Pt $4f_{7/2}$ and Ru $3p_{3/2}$, which coincides with the results obtained from the EDS spectrum.

Kucernak et al. reported the synthesis of mesoporous Pt−Ru alloy microspheres from a LLC templating mixture prepared by heating-aging processes.[14c] It was reported that a high content of O was detected in the resultant mesoporous Pt−Ru alloy by EDX attached to SEM (EDX data were not given in the manuscript[14c]) and claimed that the RuO_2 phase was mixed with a Pt−Ru fcc structure in the pore wall.[14c] The results reported by them are quite different from those obtained in this study. The mesoporous Pt−Ru alloy particles obtained in this study are not oxidized, and the pore wall is composed of one phase (a fcc structure) as a substitutional solid solution where Pt atoms were replaced by Ru atoms. The reason for this difference is not clear at the moment, but the soft-process through a solvent evaporation reported here can prevent the formation of Ru oxides.

Our process of the LLC formation through the solvent evaporation is fundamentally different from the conventional EISA method[26] which has been utilized for the formation of mesoporous silica films. In the present system, a homogeneous precursor solution composed of soluble Pt and Ru species and surfactant dissolved in water/ethanol is initially prepared, and then preferential evaporation of ethanol accelerates to form LLC mesophases. During this formation process of LLC, no reactions among Pt and Ru complexes occur, and these complexes are stabilized in the aqueous domain of LLC before electrodeposition. In contrast, in the EISA method, the polymerization of inorganic species occurs simultaneously during the solvent evaporation, in which the various interactions between the species and surfactants are inevitable.[26] Therefore, several types of phase transformation of mesoporous silica (e.g., hexagonal (*p*6*mm*) to cubic ($Ia\bar{3}d$), and cubic ($Ia\bar{3}d$) to lamellar) have been reported, depending on the experimental conditions.

In the present system, the final LLC mesophases after preferential evaporation of ethanol can be directly predicted by a certain phase diagram of ternary compositions (surfactant/water/metal species) independent of the amount of ethanol as solvent. The amount of solvent does not influence the final structure of the LLC mesophase at all. In fact, the XRD patterns of the LLC mesophases after the solvent evaporation are not changed at all, irrespective of the amount of ethanol.

For the preparation of mesoporous Pt−Ru particles, the LLC via solvent evaporation was used as direct templates. In the direct templating, it is possible to predict the final structures after metal deposition from the original LLC mesophases. For example, if a LLC mesophase used as a template takes a 2D-hexagonal structure, the deposited material has a mesoporous structure with 2D-hexagonal symmetry. The same situation can also be applied to other phases, such as cubic ($Ia\bar{3}d$) and lamellar. In these cases, the LLC mesophases act as true templates; i.e., final materials are directly templated by the LLC mesophases which are formed through solvent evaporation.

Consequently, our process is quite different from the conventional EISA method. To distinguish the difference between the conventional EISA method and ours, we newly name our process as "evaporation-mediated direct templating (EDIT)".

Conclusion

Mesoporous Pt−Ru alloy particles with an enhanced ordering were prepared via the EDIT method. The atomic crystallinity and the elemental distribution in the pore wall have been fully characterized. The pore wall is composed of a single phase (fcc structure) as a substitutional solid solution where Pt atoms were partly replaced by Ru atoms. Both elements of Pt and Ru are uniformly distributed in the pore wall. In other words, mesoporous Pt−Ru alloy obtained in this study possesses a doubly ordered structure on both meso and atomic scales. The accurate structural information obtained in this study is very important from the viewpoints of the various properties including electrochemical and catalytic performances. This paper also provides another example of mesoporous materials with crystallike wall structures.[27] Another important point is that the EDIT method can provide one-pot formation of high-quality LLC with a long-range ordering without heating-aging processes.[10−18] The EDIT method will be applicable to the deposition of various metals and alloys and even multicomponent alloys, which will be reported in the near future.

Acknowledgment. We greatly appreciate a reviewer's comment on the definition of our method and EISA. The comment by Prof. G. S. Attard (University of Southampton,

(26) (a) Ogawa, M. *J. Am. Chem. Soc.* **1994**, *116*, 7941−7942. (b) Ogawa, M. *Chem. Commun.* **1996**, 1149−1150. (c) Ogawa, M. *Langmuir* **1997**, *13*, 1853−1855. (d) Ogawa, M.; Igarashi, T.; Kuroda, K. *Bull. Chem. Soc. Jpn.* **1997**, *70*, 2833−2837. (e) Lu, Y. F.; Ganguli, R.; Drewien, C. A.; Anderson, M. T.; Brinker, C. J.; Gong, W. L.; Guo, Y. X.; Soyez, H.; Dunn, B.; Huang, M. H.; Zink, J. I. *Nature* **1997**, *389*, 364−368. (f) Brinker, C. J.; Lu, Y. F.; Sellinger, A.; Fan, H. Y. *Adv. Mater.* **1999**, *11*, 579−585. (g) Yoshikawa, T.; Nakamura, T.; Kuroda, K.; Ogawa, M. *Bull. Chem. Soc. Jpn.* **2002**, *75*, 2589−2594. (h) Shimura, N.; Ogawa, M. *Bull. Chem. Soc. Jpn.* **2004**, *77*, 1599−1606.

(27) (a) Yang, P. D.; Zhao, D. Y.; Margolese, D. I.; Chmelka, B. F.; Stucky, G. D. *Nature* **1998**, *396*, 152−155. (b) Liu, Y.; Zhang, W. Z.; Pinnavaia, T. J. *Angew. Chem., Int. Ed.* **2001**, *40*, 1255−1258. (c) Lee, B.; Lu, D. L.; Kondo, J. N.; Domen, K. *Chem. Commun.* **2001**, 2118−2119. (e) Katou, T.; Lee, B.; Lu, D. L.; Kondo, J. N.; Hara, M.; Domen, K. *Angew. Chem., Int. Ed.* **2003**, *42*, 2382−2385. (f) Li, D. L.; Zhou, H. S.; Honma, I. *Nat. Mater.* **2004**, *3*, 65−72. (g) Fang, Y.; Hu, H. *J. Am. Chem. Soc.* **2006**, *128*, 10636−10637.

Southampton, U.K.) on this point is also greatly appreciated. We acknowledge Prof. Dr. T. Osaka and Dr. T. Momma (Applied Physical Chemistry Laboratory, Waseda University) for valuable discussion and continuous encouragement. We also acknowledge Dr. C. W. Wu (Waseda University), Mr. M. Fuziwara (Kagami Memorial Laboratory for Materials Science and Technology, Waseda University), and Dr. Y. Honda (Consolidated Research Institute for Advanced Science and Medical Care, Waseda University) for HR-SEM and TEM observations. Finally we also acknowledge Ms. K. Matsui (Environmental Safety Center) for ICP analysis and Ms. A. Takai, Mr. R. Sebata, Mr. M. Sawada, and Mr. H. Kitoh (Waseda University) for experimental supports. The EDS mapping was supported by the "Nanotechnology Support Project" from the Ministry of Education, Culture, Sports, Science, and Technology (MEXT), Japanese Government. This work is supported in part by the 21st Century COE Program "Practical NanoChemistry" and Encouraging Development Strategic Research Centers Program "Establishment of Consolidated Research Institute for Advanced Science and Medical Care" from MEXT. This work is also supported by the A3 Foresight Program "Synthesis and Structural Resolution of Novel Mesoporous Materials" from the Japan Society for the Promotion of Science (JSPS). Y.Y. is grateful for financial support via a Grant-in-Aid for JSPS Fellows from MEXT.

Supporting Information Available: Figure S1, showing TEM images of aggregated particles with two types of TEM images of the same aggregated particles taken by changing tilt angles, Figure S2, showing dark-field TEM images of aggregated particles, and Figure S3, showing highly magnified TEM images of the square areas of (A) and (B) in Figure S1, respectively. This material is available free of charge via the Internet at http://pubs.acs.org.

CM062539N